

Chromatin-associated RNA interference components contribute to transcriptional regulation in *Drosophila*

Filippo M. Cernilogar^{1,2†*}, Maria Cristina Onorati^{3*}, Greg O. Kothe⁴, A. Maxwell Burroughs⁵, Krishna Mohan Parsi^{1,2}, Achim Breiling⁶, Federica Lo Sardo¹, Alka Saxena⁵, Keita Miyoshi⁷, Haruhiko Siomi⁷, Mikiko C. Siomi^{7,8}, Piero Carninci⁵, David S. Gilmour⁴, Davide F. V. Corona³ & Valerio Orlando¹

RNA interference (RNAi) pathways have evolved as important modulators of gene expression that operate in the cytoplasm by degrading RNA target molecules through the activity of short (21–30 nucleotide) RNAs^{1–6}. RNAi components have been reported to have a role in the nucleus, as they are involved in epigenetic regulation and heterochromatin formation^{7–10}. However, although RNAi-mediated post-transcriptional gene silencing is well documented, the mechanisms of RNAi-mediated transcriptional gene silencing and, in particular, the role of RNAi components in chromatin dynamics, especially in animal multicellular organisms, are elusive. Here we show that the key RNAi components Dicer 2 (DCR2) and Argonaute 2 (AGO2) associate with chromatin (with a strong preference for euchromatic, transcriptionally active, loci) and interact with the core transcription machinery. Notably, loss of function of DCR2 or AGO2 showed that transcriptional defects are accompanied by the perturbation of RNA polymerase II positioning on promoters. Furthermore, after heat shock, both *Dcr2* and *Ago2* null mutations, as well as missense mutations that compromise the RNAi activity, impaired the global dynamics of RNA polymerase II. Finally, the deep sequencing of the AGO2-associated small RNAs (AGO2 RIP-seq) revealed that AGO2 is strongly enriched in small RNAs that encompass the promoter regions and other regions of heat-shock and other genetic loci on both the sense and antisense DNA strands, but with a strong bias for the antisense strand, particularly after heat shock. Taken together, our results show that DCR2 and AGO2 are globally associated with transcriptionally active loci and may have a pivotal role in shaping the transcriptome by controlling the processivity of RNA polymerase II.

Accumulating evidence indicates that RNAi components and small RNAs function in the nucleus to control heterochromatin formation, as well as repeat-induced gene silencing and transposable element mobilization^{7–10}. However, the global association of RNAi components with chromatin and their role in transcriptional regulation remains to be elucidated. To investigate a role for RNAi in the chromatin dynamics of a multicellular organism and, possibly, in transcriptional gene silencing, we first determined whether any of the key RNAi components are present in the nucleus of *Drosophila* cells. Cellular fractionation of embryonic tissue culture cells (S2 cells) showed that the microRNA-processing factors DCR1 and AGO1, as well as the RNAi component AGO2, are equally distributed between the cytoplasm and the nucleus (Supplementary Fig. 1a). By contrast, the RNAi protein DCR2 is greatly enriched in the nuclear fraction (Supplementary Fig. 1a). To evaluate the association of RNAi components with the different nuclear compartments, we carried out chromatin fractionation experiments¹¹ (Supplementary Fig. 1b, c). A substantial amount of

DCR2 and AGO2 was detected in chromatin fractions, together with RNA polymerase II (RNA Pol II), Negative elongation factor E (NELF-E), Polycomb (Pc) and histone H3 (Supplementary Fig. 1c). By contrast, most of the cellular DCR1 and AGO1 was found in the Triton X-100 soluble fraction (S1 fraction), together with tubulin, a marker for proteins that are not associated with chromatin (Supplementary Fig. 1c). Taken together, our data indicate that the DCR2–AGO2 complex is mainly associated with chromatin, whereas the DCR1–AGO1 complex is mostly cytoplasmic, in accordance with its cytoplasmic function (that is, post-transcriptional gene silencing).

To determine whether RNAi components associate with chromatin *in vivo*, *Drosophila* polytene chromosomes were stained with AGO2- and DCR2-specific monoclonal antibodies^{3,12,13}. Both AGO2 and DCR2 were detected at several hundred sites on polytene chromosomes from wild-type larvae (Supplementary Figs 1d, g and 2a, b). By contrast, little or no staining was detected in *Ago2*- or *Dcr2*-null chromosomes¹² (Supplementary Fig. 1f, i and Supplementary Table 1a). Strikingly, the majority of AGO2- and DCR2-associated loci correspond to interbands, suggesting that AGO2 and DCR2 preferentially associate with euchromatic, transcriptionally active, loci¹⁴ (Supplementary Fig. 2a, b). In particular, the chromatin binding of DCR2 requires AGO2, but the converse is not true (Supplementary Fig. 3), suggesting that AGO2 also acts as the RNAi effector complex on chromatin.

Interestingly, AGO2 and DCR2 are present at the 87A and 87C cytogenetic loci (Supplementary Fig. 1e, h). These cytogenetic loci contain copies of the heat-shock gene *Hsp70*, thus providing well-characterized inducible candidate genes with which to investigate the role of DCR2 and AGO2 in transcription and, in particular, in RNA Pol II pausing regulation^{15,16}. To determine whether DCR2 and AGO2 affect *Hsp70* transcription, *Hsp70* transcript levels were measured in control cells and in cells depleted of DCR2 or AGO2 (Supplementary Fig. 4). The knockdown of either RNAi component resulted in a significant increase in *Hsp70* transcripts in non-heat-shocked cells (Fig. 1a, b). Similar results were obtained for a second heat-shock gene, *Hsp68* (Fig. 1a, b). The increased expression of *Hsp70* and *Hsp68* in cells depleted of DCR2 could be reversed by the expression of a Flag-tagged wild-type copy of DCR2 (DCR2–Flag) (Fig. 1c), indicating that the change in expression was not the result of an off-target effect of the *Dcr2* RNAi. Interestingly, the levels of the endogenous AGO2 protein increased together with the expression of wild-type DCR2–Flag (Supplementary Fig. 4a), suggesting that the DCR2–Flag protein is integrated into the RNAi pathway and that re-establishment of functional levels of DCR2 and AGO2 rescues the observed transcriptional defects in heat-shock genes. However, the depletion of DCR2 and AGO2 did not affect the expression of *Hsp70* and *Hsp68*

¹Dulbecco Telethon Institute, Epigenetics and Genome Reprogramming, IRCCS Fondazione Santa Lucia, Via del Fosso di Fiorano 64, 00143 Rome, Italy. ²Dulbecco Telethon Institute, IGB ABT-CNR, Via Pietro Castellino 111, 80131 Naples, Italy. ³Dulbecco Telethon Institute at Università degli Studi di Palermo, Dipartimento STEMBO, Sezione Biologia Cellulare, Viale delle Scienze, Edificio 16, 90128 Palermo, Italy. ⁴Department of Biochemistry and Molecular Biology, Center for Eukaryotic Gene Regulation, The Pennsylvania State University, University Park, Pennsylvania 16802, USA. ⁵RIKEN Omics Science Center, RIKEN Yokohama Institute, 1-7-22 Suehiro-cho, Tsurumi-ku, Yokohama, Kanagawa 230-0045, Japan. ⁶Division of Epigenetics, DKFZ-ZMBH Alliance, German Cancer Research Center, Im Neuenheimer Feld 580, 69120 Heidelberg, Germany. ⁷Keio University School of Medicine, Tokyo 160-8582, Japan. ⁸JST, CREST, Saitama 332-0012, Japan. †Present address: Helmholtz Center Munich, Institute of Developmental Genetics, Ingolstaedter Landstrasse 1, 85764 Munich-Neuherberg, Germany.

*These authors contributed equally to this work.

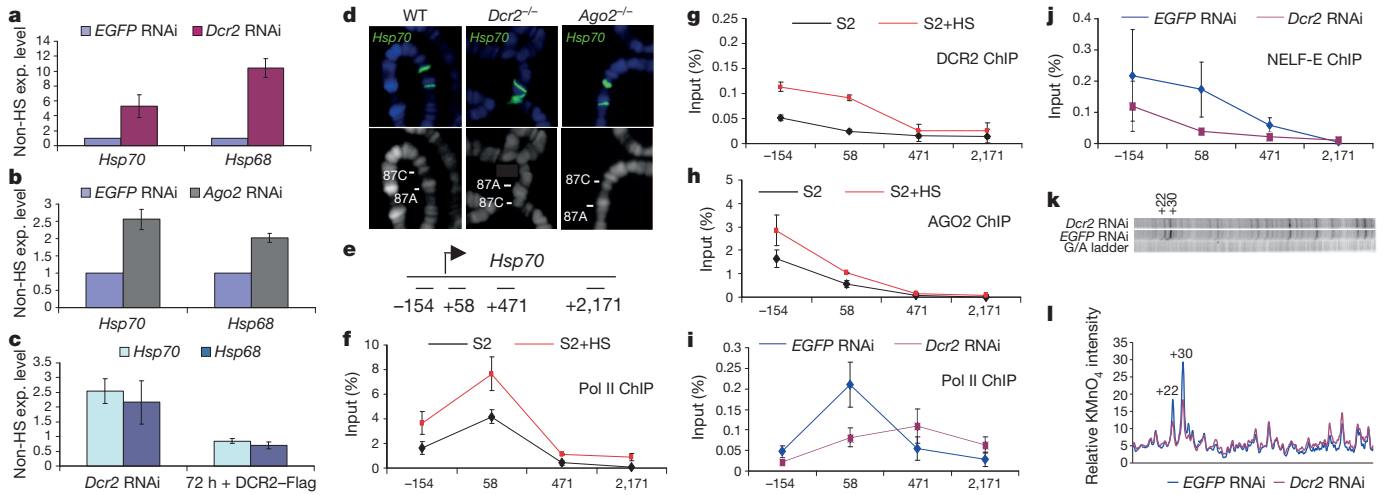


Figure 1 | RNA Pol II promoter-proximal pausing on *Hsp70* is decreased in cells treated with *Dcr2* RNAi. **a, b**, Quantitative RT-PCR analysis of heat-shock (HS) gene transcripts. RNA from S2 cells treated with enhanced green fluorescent protein (*EGFP*) dsRNA (control), *Dcr2* dsRNA (**a**) or *Ago2* dsRNA (**b**) was analysed with primers specific for the indicated heat-shock genes. **c**, Induction of the *Dcr2-Flag* transgene is able to revert the phenotype induced by DCR2 depletion. S2 cells that had been stably transformed with a *Dcr2-Flag* transgene were treated with *EGFP* dsRNA (control) or *Dcr2* dsRNA. *Dcr2-Flag* expression was induced only in the *Dcr2* RNAi sample, by the addition of copper. The samples were analysed before and after a 72-h induction of the transgene. The transcript levels are shown with respect to the *EGFP* control (experiment:control ratio); $n = 3$. The bars represent the mean \pm s.d. **d**, *Hsp70* DNA-FISH on polytene chromosomes from wild type (WT), homozygous *Dcr2^{L811fsX}* (*Dcr2^{-/-}*) or homozygous *Ago2⁴¹⁴* (*Ago2^{-/-}*) mutant larvae, showing the merge of DNA (blue) and FISH (green) signals (top) and DNA staining (bottom). **e**, Schematic representation of the *Hsp70* transcription unit with the position of the PCR amplicons used in this study. The numbers indicate the middle of each amplicon with respect to the transcription start site (arrow). **f-h**, ChIP analysis of the heat-shock gene *Hsp70*. Chromatin from S2

during heat shock, suggesting that RNAi activity is not involved in heat-shock-gene-mediated activation (Supplementary Fig. 5a, b).

Typically, the activation of heat-shock genes results in the chromosome decondensation of heat-shock loci, forming large puffs on polytene chromosomes¹⁷. Therefore, we used DNA fluorescence *in situ* hybridization (DNA-FISH) to look at the chromatin structure of heat-shock loci in polytene chromosomes with specific null mutations of *Dcr2* and *Ago2*: *Dcr2^{L811fsX}* and *Ago2⁴¹⁴*. Interestingly, we observed that the 87C locus is partially decondensed in *Dcr2^{L811fsX}* and *Ago2⁴¹⁴* mutant chromosomes relative to the wild-type controls (Fig. 1d). The 87C locus contains four copies of *Hsp70* distributed over 30 kilobases. Decondensation was not evident at 87A, probably because this locus has only two copies of *Hsp70* within a region of less than 10 kilobases.

Because the data from PCR following reverse transcription (RT-PCR) and from cytogenetic analyses suggested that the maintenance of RNA Pol II pausing was defective, we used chromatin immunoprecipitation (ChIP) to measure the level of RNA Pol II with a phosphorylated Ser-5 residue that was present on the *Hsp70* gene before and after heat shock (Fig. 1e, f). The primers used for quantitative PCR analysis of the immunoprecipitated DNA spanned several regions of the *Hsp70* gene. An upstream primer set centred at -154 bases from the transcription start site was used to detect the heat-shock element; the +58 primer set encompassed the region of the paused polymerase¹⁸; and two other primer sets were downstream within the transcription unit, extending towards the end of the gene (Fig. 1e). Consistent with previous observations¹⁸, the RNA Pol II profile observed in S2 cells showed a peak in the region of paused RNA Pol II (+58 primer set) (Fig. 1f), which increased after heat shock. Furthermore, ChIP analysis showed that DCR2 and AGO2 were present at the *Hsp70* promoter region (-154/+58) (Fig. 1g, h and Supplementary Fig. 6). Interestingly, after heat

shock, the levels of both DCR2 and AGO2 proteins increased in the *Hsp70* promoter region (Fig. 1g, h, Supplementary Figs 1i, 6 and Methods). Consistent with RT-PCR and cytogenetic data, DCR2 depletion consistently decreased the level of RNA Pol II on *Hsp70* in the region of the paused polymerase (primer set +58) (Fig. 1i). We extended our ChIP analysis to the NELF-E protein, which is part of the transcriptional regulatory complex that causes RNA Pol II pausing^{16,19}. Depletion of DCR2 caused the level of NELF-E on *Hsp70* to decrease in the +58 region, where RNA Pol II pauses (Fig. 1j). The total cellular levels of RNA Pol II and NELF-E protein were not altered by DCR2 depletion (Supplementary Fig. 4b), indicating that the diminished level of RNA Pol II and NELF-E detected on *Hsp70* is not a consequence of a decrease in the amount of available protein. Conversely, in DCR2-depleted cells, we observed a reduction in the level of the AGO2 protein (Supplementary Fig. 4b). This was not simply a result of cross-targeting of the double-stranded RNA (dsRNA) because the level of the *Ago2* transcript was unaffected (Supplementary Fig. 4c). Likewise, *Ago2* dsRNA resulted in reduced DCR2 protein levels (Supplementary Fig. 4d) without affecting *Dcr2* messenger RNA levels (Supplementary Fig. 4e). These results suggest that DCR2 and AGO2 stabilize each other in a protein complex that is important for repressing heat-shock genes in uninduced cells. To confirm that DCR2 depletion affected RNA Pol II pausing on *Hsp70*, we carried out permanganate footprinting analysis. Permanganate reacts with thymine bases in regions of single-stranded DNA, revealing the presence and location of transcriptionally engaged RNA Pol II. We observed a significant reduction in permanganate reactivity of thymine residues at +22 and +30 of *Hsp70* in DCR2-depleted cells (Fig. 1k, l), which is in agreement with the reduced occupancy of the DNA by RNA Pol II in this region (primer set +58) that was shown by ChIP (Fig. 1i).

Hence, DCR2 is involved in maintaining paused RNA Pol II at the observed *Hsp70* loci.

Heat-shock gene expression and loss of paused RNA Pol II on depletion of DCR2 could be a consequence of stress induced by depletion of the RNAi machinery in the cell. Therefore, we evaluated the impact of perturbing the RNAi pathway on the transcription of non-heat-shock genes. Four non-heat-shock genes (*CG9008*, *fz*, *rho* and *mfas*) that have paused RNA Pol II were analysed by permanganate footprinting^{19,20}. Depletion of DCR2 was found also to alter the distribution of RNA Pol II in the promoter-proximal region of these genes (Supplementary Fig. 7). These changes were also accompanied by differences in transcript levels (Supplementary Fig. 8). Notably, the observed changes in RNA Pol II resulted both in upregulation (for *CG9008*, *fz* and *rho*) and downregulation (*mfas*) of the corresponding transcripts (Supplementary Fig. 8). Thus, the RNAi machinery can influence RNA Pol II pausing at non-heat-shock genes, arguing against a nonspecific DCR2-induced heat-shock response.

During heat shock, most of the *Drosophila* genome is transcriptionally quiescent. The elongating RNA Pol II dissociates from euchromatic interbands and accumulates at heat-shock loci²¹. We used this dynamic RNA Pol II relocalization behaviour to follow the chromatin binding and distribution of elongating RNA Pol II (which is Ser-2-phosphorylated), as well as AGO2 and DCR2, *in vivo*. In agreement with the ChIP results (Fig. 1h), we found that, after heat shock, AGO2 accumulated at heat-shock loci (Fig. 2a). However, in contrast to RNA Pol II, the association of AGO2 with other loci appears unchanged (Fig. 2a). When we analysed the dynamic chromatin repositioning of RNA Pol II after heat shock in *Ago2*-null mutant chromosomes, we found that RNA Pol II was still accumulated at the heat-shock loci (Fig. 2b). Strikingly, a substantial fraction of elongating RNA Pol II in *Ago2*^{A14} mutants was retained at many euchromatic sites after heat shock (Fig. 2b). The same behaviour was observed for the *Dcr2*^{L811fSX} mutant (Supplementary Table 2). Taken together, these results show that AGO2 and DCR2 associate with many euchromatic sites and that their activity is probably required for the correct execution of global transcriptional repression after heat shock.

To dissect the role of RNAi in RNA Pol II regulation, we used three mutants that each carried a single amino acid substitution affecting the following RNAi activities: the helicase (*Dcr2*^{L188F}), the dicing (*Dcr2*^{P1496L}) and the AGO2 slicing (*Ago2*^{V966M}) activities^{22,23} (Supplementary Table 1a). To check for DCR2- and AGO2-specific requirements, we first used DNA-FISH to analyse chromosome decondensation at *Hsp70* loci. Puffing frequencies were increased in all three mutants, particularly in the AGO2 slicing mutant (*Ago2*^{V966M}) (Supplementary Table 1b). In addition, in all of these mutants, the *Hsp70A*, *Hsp70B* and *Hsp68* transcripts were present at increased levels before heat shock, compared with wild type (Supplementary Fig. 9). Interestingly, the transcript increase was also evident at 87A (*Hsp70A*), where the chromatin decondensation was not appreciable at a cytogenetic level (Supplementary Fig. 9 and Supplementary Table 1b). Thus, all tested mutants induced transcript upregulation of the *Hsp70* genomic region, although this was not always accompanied by chromatin decondensation. The uncoupling of chromatin decondensation and transcriptional activation has been reported previously²⁴, although in this case we cannot exclude an RNAi-dependent post-transcriptional mechanism influencing the *Hsp70A* transcript levels.

Next, we analysed RNA Pol II distribution and dynamics on polytene chromosomes in the same *Dcr2* and *Ago2* mutants. Remarkably, although with a different degree of penetrance, all three mutants failed to relocalize elongating RNA Pol II after heat shock (Fig. 2c–f and Supplementary Table 2), suggesting that RNAi enzymatic activity is involved in the global RNA Pol II dynamics following the heat-shock stress response.

The association of RNAi components with RNA Pol II complexes has been reported in other systems^{25–27}. To investigate the possibility that these proteins are part of a complex that regulates RNA Pol II

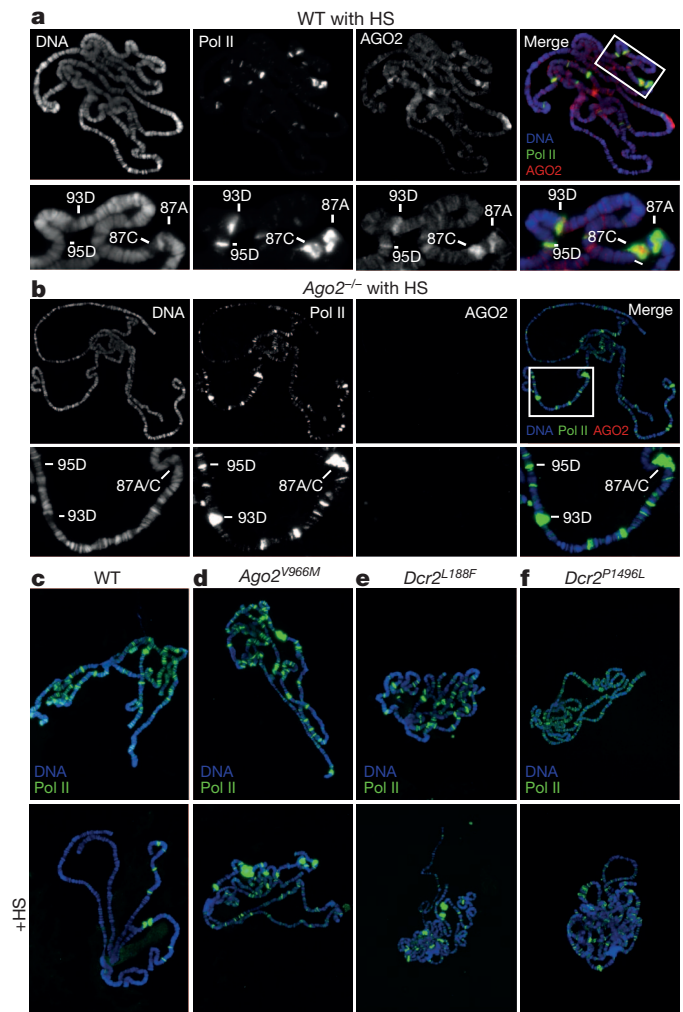


Figure 2 | Chromatin localization of RNA Pol II and AGO2 after heat shock. **a, b**, Co-immunolocalization of AGO2 (red) and elongating RNA Pol II (green) in WT (**a**) and homozygous *Ago2*^{A14} (*Ago2*^{-/-}) mutant chromosomes (**b**) after heat shock (HS). DNA is stained in blue. Single signals are shown in black and white. The bottom row shows a higher magnification of the boxed area (top right). **c–f**, Immunolocalization of elongating RNA Pol II (green) in WT (**c**) and homozygous *Ago2*^{V966M} (**d**), homozygous *Dcr2*^{L188F} (**e**) and homozygous *Dcr2*^{P1496L} (**f**) chromosomes shows that missense mutations in DCR2 or AGO2 influence the behaviour of elongating RNA Pol II. DNA is stained in blue. Chromosomes in the bottom panel have been exposed to heat shock.

elongation, thus establishing a link with the observed ‘pausing’ defects, we tested for interactions between DCR2, NELF-E and RNA Pol II in nuclear extracts derived from *Drosophila* S2 cells. Immunoprecipitated fractions were evaluated by western blotting for the presence of RNA Pol II, DCR2, AGO2 and NELF-E (Fig. 3a). As expected, DCR2 interacted with AGO2 (ref. 28) (Fig. 3a). In addition, we found that DCR2 and AGO2 interacted with RNA Pol II and NELF-E (Fig. 3a). All of these interactions were resistant to RNase treatment, indicating that they are not an indirect consequence of protein trapping associated with emerging RNA molecules (Supplementary Fig. 10a). Compared with general transcription factors, the amount of RNA Pol II interacting with DCR2 seems to be in the same range as for the TATA-binding protein (TBP), confirming the association of DCR2 with many active loci on polytene chromosomes (Fig. 3b). When we tested the same interaction in DCR2-depleted cells, we observed a decrease in the levels of NELF-E and AGO2 associated with RNA Pol II (Supplementary Fig. 10b). These observations indicate that the DCR2–AGO2 complex influences the association of NELF-E with RNA Pol II, thereby providing a possible explanation for the observation that the

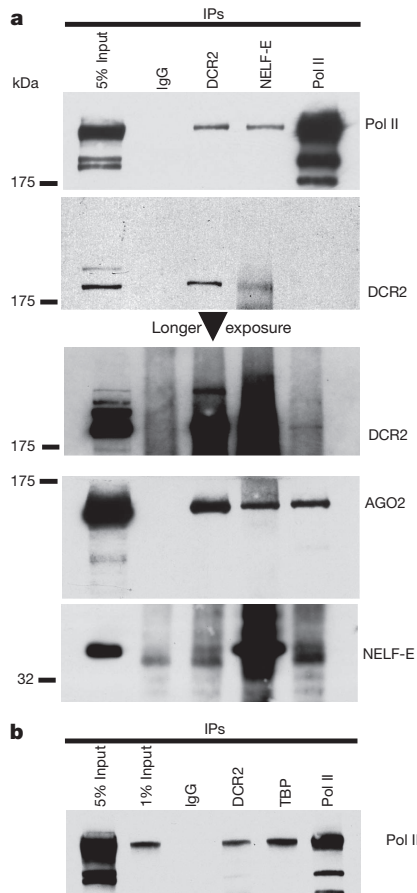


Figure 3 | DCR2 and the RNAi effector protein AGO2 associate with RNA Pol II and NELF-E. **a**, Nuclear extracts from *Drosophila* S2 cells were immunoprecipitated with antibodies specific for the indicated proteins (with IgG as a negative control, top), and the immunoprecipitates (IPs) were analysed by western blotting for the presence of RNA Pol II, DCR2, AGO2 and NELF-E proteins. **b**, Nuclear extracts from S2 cells were immunoprecipitated with antibodies specific for the indicated proteins (with IgG as a negative control, top) and analysed by western blotting for the presence of RNA Pol II.

depletion of DCR2 alters the behaviour of RNA Pol II in the promoter-proximal region of several genes.

Our data indicate an involvement of the RNAi machinery in the heat-shock stress response. To evaluate possible heat-shock-induced changes in the expression signature of AGO2-dependent small RNAs, we sequenced small RNAs bound to AGO2 before and after heat shock. Small RNA libraries from S2 cells were generated from RNA fractions obtained by immunoprecipitation with antibodies against AGO2 or with control IgG, with or without heat shock (Supplementary Fig. 11). Basic statistical parameters for the four libraries are listed in Supplementary Table 3. Many sequenced tags mapped to repeat regions in more than one location (Supplementary Fig. 12), which is consistent with previous *Drosophila* deep-sequenced AGO2-immunoprecipitation libraries^{3,5}. First, we focused our attention on the heat-shock promoter regions (500 base pairs (bp) upstream and 50 bp downstream of the transcription start site). We found that heat-shock loci promoter regions were enriched in small RNAs and showed a marked increase in small RNA enrichment on heat shock. This was most noticeable for *Hsp23* and for all *Hsp70* loci (Supplementary Tables 4 and 5). This observation prompted us to consider whether the level of small RNAs increased across all promoters²⁹. Strikingly, the most enriched promoters were the *Hsp70B* loci, and *Hsp23* was also one of the 20 most enriched loci, suggesting a direct role for AGO2 at these promoters (Fig. 4a). The possible function or role in the heat-shock response of other loci present in the top 20 list is not known.

Next, we tried to gauge shifts in small RNA tags derived from discrete transcribed regions at all gene loci in response to heat shock (Supplementary Fig. 14a). We observed little or no relative enrichment along different length intervals, suggesting that these tags are not derived exclusively from promoter regions but are equally distributed along the transcription unit (Supplementary Fig. 13). Although there was a sharp increase in AGO2-associated small RNAs in the heat-shock condition relative to the heat-shock condition negative control immunoprecipitation (confirming the specific association of these tags with AGO2), only a small increase was observed in the heat-shock condition AGO2 immunoprecipitation relative to the normal condition AGO2 immunoprecipitation, suggesting that these transcript-associating tags are present even under normal conditions (Supplementary Fig. 14a). These data suggest a role for AGO2 in regulating RNA Pol II processivity, in addition to promoter regulation.

We then analysed the strand bias of AGO2-associated small RNAs. Sense and antisense tags had a specular distribution within individual libraries, with the ratio of the sums of the sense and antisense small RNA tag counts mapping to heat-shock loci and the set of all *Drosophila* genes being equal to approximately 1 (Supplementary Fig. 14b). However, a comparison of normalized sense and antisense tag counts across AGO2-immunoprecipitation and negative-control-immunoprecipitation libraries showed a pronounced enrichment in antisense tags and little or no enrichment in sense tags, suggesting that antisense tags are highly specific in their association with AGO2 but that

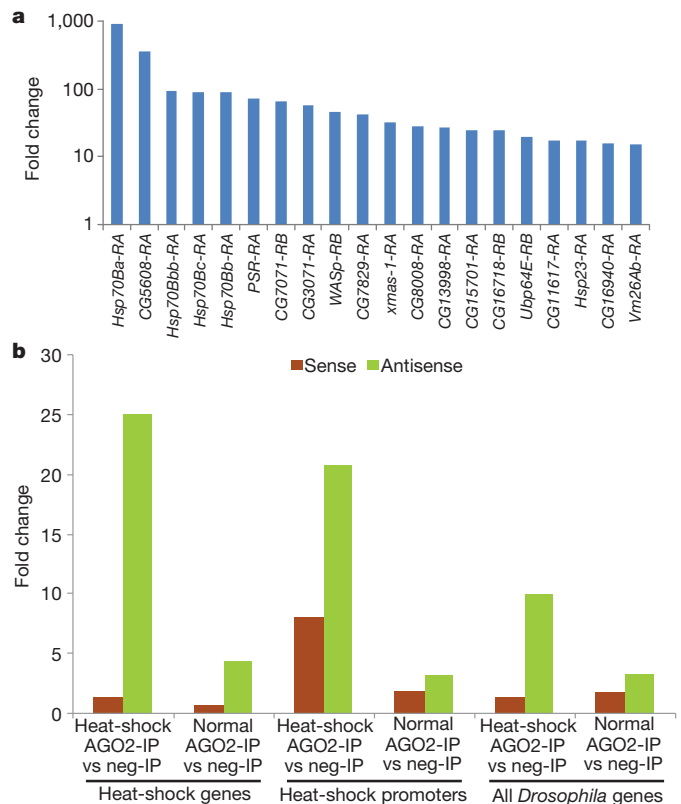


Figure 4 | Features of AGO2-associated small RNAs. **a**, The 20 promoters that are the most enriched in small RNAs under heat-shock versus non-heat-shock (normal) conditions. A comparison of the small RNA fold enrichment in the AGO2-immunoprecipitation (AGO2-IP) libraries between normal and heat-shock conditions is shown for all promoters. **b**, Relative enrichment calculated as fold change (y-axis) for the sum of all sense or antisense tags across different conditions. The analysed gene/promoter definitions and conditions are labelled below the graph. Little to no sense tag enrichment is observed across gene/promoter definitions, whereas antisense tags show enrichment across the groups, particularly under heat-shock conditions. Neg-IP, negative control immunoprecipitation.

sense tags are not. Additionally, the observed enrichment implies that antisense tag association is strongest in the heat-shock condition (Fig. 4b).

Next, we examined cap analysis of gene expression (CAGE) data that had been generated in *Drosophila* embryos for the modENCODE project²⁹, to survey the extent of antisense transcriptional activity at heat-shock loci (Supplementary Table 6). Antisense transcriptional activity was observed at almost all heat-shock loci and, surprisingly, many *Hsp70* loci had roughly equivalent levels of sense and antisense transcription (Supplementary Table 6), suggesting a possible source for the observed small RNA tags. Taken together, these data indicate that the observed small RNAs are probably derived from dsRNA precursors and that sequences that are antisense to the loci preferentially associate with AGO2, implying that sense targeting occurs.

In this study, we show that, in *Drosophila*, RNAi components operate in the nucleus, associate with transcriptionally active (rather than inactive) gene loci, interact with RNA Pol II and contribute to transcriptional control in a multicellular organism, particularly during the heat-shock stress response. Our results reveal that RNAi function has also evolved as a key nuclear pathway that operates in the context of pervasive sense and antisense transcription to regulate RNA-level homeostasis in the cell (see also Supplementary Discussion).

METHODS SUMMARY

Wild-type *Drosophila melanogaster* (Canton-S or *w¹¹¹⁸*) and the mutant stocks *Dcr2^{L811fsX}*, *Ago2^{V966M}*, *Ago2^{A14}*, *Dcr2^{L188F}* and *Dcr2^{P1496L}* (refs 1, 2, 22, 23) were maintained under standard conditions. S2 cells were grown in serum-free insect culture medium. Protein–protein interactions were analysed by immunoprecipitations from nuclear extracts with specific antibodies. The production of dsRNAs was performed *in vitro* by T7 transcription, and the dsRNAs were transfected into S2 cells using FuGENE reagent (Roche). ChIP experiments were performed using formaldehyde-crosslinked chromatin from S2 cells. ChIP-purified DNA was analysed by using quantitative PCR with primer pairs specific for the *Hsp70* locus. Total RNA from S2 cells or larvae was reverse transcribed and analysed by quantitative PCR. Polytene chromosomes were prepared from third-instar larvae grown at 18 °C and were used for FISH. FISH signals were quantified by densitometric analysis using QFluoro software (Leica). To analyse RNA Pol II pausing on the promoters of *Hsp70* and non-heat-shock genes in S2 cells, permanganate footprinting was used. AGO2-associated RNAs were isolated from S2 cells as previously described⁶. Small RNA libraries were prepared and sequenced using a Genome Analyzer Iix (Illumina) in two lanes. For additional details see the Methods.

Full Methods and any associated references are available in the online version of the paper at www.nature.com/nature.

Received 13 July 2009; accepted 17 August 2011.

Published online 6 November 2011.

- Okamura, K., Ishizuka, A., Siomi, H. & Siomi, M. C. Distinct roles for Argonaute proteins in small RNA-directed RNA cleavage pathways. *Genes Dev.* **18**, 1655–1666 (2004).
- Lee, Y. S. *et al.* Distinct roles for *Drosophila* Dicer-1 and Dicer-2 in the siRNA/miRNA silencing pathways. *Cell* **117**, 69–81 (2004).
- Kawamura, Y. *et al.* *Drosophila* endogenous small RNAs bind to Argonaute 2 in somatic cells. *Nature* **453**, 793–797 (2008).
- Ghildiyal, M. *et al.* Endogenous siRNAs derived from transposons and mRNAs in *Drosophila* somatic cells. *Science* **320**, 1077–1081 (2008).
- Czech, B. *et al.* An endogenous small interfering RNA pathway in *Drosophila*. *Nature* **453**, 798–802 (2008).
- Okamura, K. *et al.* The *Drosophila* hairpin RNA pathway generates endogenous short interfering RNAs. *Nature* **453**, 803–806 (2008).
- Allshire, R. C. & Karpen, G. H. Epigenetic regulation of centromeric chromatin: old dogs, new tricks? *Nature Rev. Genet.* **9**, 923–937 (2008).
- Malone, C. D. & Hannon, G. J. Small RNAs as guardians of the genome. *Cell* **136**, 656–668 (2009).
- Moazed, D. Small RNAs in transcriptional gene silencing and genome defence. *Nature* **457**, 413–420 (2009).
- Teixeira, F. K. *et al.* A role for RNAi in the selective correction of DNA methylation defects. *Science* **323**, 1600–1604 (2009).
- Llano, M. *et al.* Identification and characterization of the chromatin-binding domains of the HIV-1 integrase interactor LEDGF/p75. *J. Mol. Biol.* **360**, 760–773 (2006).
- Miyoshi, K., Tsukumo, H., Nagami, T., Siomi, H. & Siomi, M. C. Slicer function of *Drosophila* Argonautes and its involvement in RISC formation. *Genes Dev.* **19**, 2837–2848 (2005).

- Miyoshi, K., Okada, T. N., Siomi, H. & Siomi, M. C. Characterization of the miRNA–RISC loading complex and miRNA–RISC formed in the *Drosophila* miRNA pathway. *RNA* **15**, 1282–1291 (2009).
- Weeks, J. R., Hardin, S. E., Shen, J., Lee, J. M. & Greenleaf, A. L. Locus-specific variation in phosphorylation state of RNA polymerase II *in vivo*: correlations with gene activity and transcript processing. *Genes Dev.* **7**, 2329–2344 (1993).
- Lis, J. T. Imaging *Drosophila* gene activation and polymerase pausing *in vivo*. *Nature* **450**, 198–202 (2007).
- Wu, C. H. *et al.* NELF and DSIF cause promoter proximal pausing on the *hsp70* promoter in *Drosophila*. *Genes Dev.* **17**, 1402–1414 (2003).
- Simon, J. A., Sutton, C. A., Lobell, R. B., Glaser, R. L. & Lis, J. T. Determinants of heat shock-induced chromosome puffing. *Cell* **40**, 805–817 (1985).
- Boehm, A. K., Saunders, A., Werner, J. & Lis, J. T. Transcription factor and polymerase recruitment, modification, and movement on *hsp70* *in vivo* in the minutes following heat shock. *Mol. Cell. Biol.* **23**, 7628–7637 (2003).
- Lee, C. *et al.* NELF and GAGA factor are linked to promoter-proximal pausing at many genes in *Drosophila*. *Mol. Cell. Biol.* **28**, 3290–3300 (2008).
- Gilchrist, D. A. *et al.* NELF-mediated stalling of Pol II can enhance gene expression by blocking promoter-proximal nucleosome assembly. *Genes Dev.* **22**, 1921–1933 (2008).
- Cai, W. *et al.* RNA polymerase II-mediated transcription at active loci does not require histone H3S10 phosphorylation in *Drosophila*. *Development* **135**, 2917–2925 (2008).
- Lim, D. H., Kim, J., Kim, S., Carthew, R. W. & Lee, Y. S. Functional analysis of dicer-2 missense mutations in the siRNA pathway of *Drosophila*. *Biochem. Biophys. Res. Commun.* **371**, 525–530 (2008).
- Kim, K., Lee, Y. S. & Carthew, R. W. Conversion of pre-RISC to holo-RISC by Ago2 during assembly of RNAi complexes. *RNA* **13**, 22–29 (2007).
- Chambeyron, S. & Bickmore, W. A. Chromatin decondensation and nuclear reorganization of the *HoxB* locus upon induction of transcription. *Genes Dev.* **18**, 1119–1130 (2004).
- Kim, D. H., Villeneuve, L. M., Morris, K. V. & Rossi, J. J. Argonaute-1 directs siRNA-mediated transcriptional gene silencing in human cells. *Nature Struct. Mol. Biol.* **13**, 793–797 (2006).
- Kavi, H. H. & Birchler, J. A. Interaction of RNA polymerase II and the small RNA machinery affects heterochromatic silencing in *Drosophila*. *Epigenetics Chromatin* **2**, 15 (2009).
- El-Shami, M. *et al.* Reiterated WG/GW motifs form functionally and evolutionarily conserved ARGONAUTE-binding platforms in RNAi-related components. *Genes Dev.* **21**, 2539–2544 (2007).
- Ghildiyal, M. & Zamore, P. D. Small silencing RNAs: an expanding universe. *Nature Rev. Genet.* **10**, 94–108 (2009).
- Hoskins, R. A. *et al.* Genome-wide analysis of promoter architecture in *Drosophila melanogaster*. *Genome Res.* **21**, 182–192 (2011).

Supplementary Information is linked to the online version of the paper at www.nature.com/nature.

Acknowledgements We are deeply grateful to P. Macino for discussions. We also thank R. Carthew, E. Lai, Q. Liu, R. Paro, Y. Sik Lee, and J. T. Kadonaga for reagents. This work was supported by grants from the following: the National Institutes of Health (GM47477) to D.S.G.; the Deutsche Forschungsgemeinschaft (SPP 1356) to A.B.; the Japan Science and Technology Agency (JSPS) through the ‘Funding Program for Next Generation World-Leading Researchers’ (NEXT Program) (a Grant-in-Aid for Scientific Research (A) No. 20241047) and the Council for Science and Technology Policy to P.C.; the NEXT Program (a Research Grant-in-Aid to the RIKEN OSC) to K.M., M.C.S. and H.S.; Core Research for Evolutional Science and Technology (CREST) from the Japan Science and Technology Agency to M.C.S.; Fondazione Telethon, the Giovanni Arpanese Harvard Foundation, FIRB-MIUR, Associazione Italiana Ricerca Cancro (AIRC), the Human Frontier Science Program CDA and the EMBO Young investigator program to D.F.V.C.; Fondazione Telethon, AIRC and the EU FP6 Epigenome Network of Excellence to V.O. This work was also made possible with the contribution of the Italian Ministry of Foreign Affairs, ‘Direzione Generale per la Promozione e la Cooperazione Culturale’ to V.O. A.S. is supported by a JSPS fellowship (ID P09745). Sequencing was provided by the Genas service (RIKEN Omics Science Center).

Author Contributions F.M.C. and V.O. conceived the study. F.M.C. and A.B. performed the ChIP experiments. F.M.C. and K.M.P. carried out the chromatin fractionation assays and the western blotting. F.M.C. carried out the quantitative RT–PCR on S2 cells. K.M.P. and F.L.S. performed the quantitative RT–PCR on mutant larvae prepared by M.C.O. F.M.C. performed the co-immunoprecipitations and contributed reagents for the chromosome and permanganate footprinting experiments. M.C.O. performed the polytene chromosome experiments. G.O.K. and D.S.G. performed the permanganate footprinting experiments. A.M.B. performed the bioinformatic analysis. A.S. and P.C. performed the deep sequencing. K.M., H.S. and M.C.S. performed the purification of the AGO2-associated small RNAs. F.M.C., M.C.O., D.S.G., D.F.V.C. and V.O. designed the experiments and interpreted the results. F.M.C., D.S.G., D.F.V.C. and V.O. wrote the manuscript with the contribution of M.C.O., A.B. and A.M.B., as well as input from the other co-authors.

Author Information Sequence data have been deposited in the DNA Data Bank of Japan under accession code DRA000418. Reprints and permissions information is available at www.nature.com/reprints. The authors declare no competing financial interests. Readers are welcome to comment on the online version of this article at www.nature.com/nature. Correspondence and requests for materials should be addressed to V.O. (vorlando@dti.telethon.it).

METHODS

Fly stocks. Flies (*Drosophila melanogaster*) were maintained under standard protocols. Canton-S or w^{1118} were used as wild-type strains. The *Dcr2*^{L811f5X} and *Ago2*^{V966M} stocks^{2,23} were obtained from R. W. Carthew. The *Ago2*^{Δ14} stock¹ was obtained from E. Lai. The *Dcr2*^{L188F} and *Dcr2*^{P1496L} stocks²² were obtained from Y. Sik Lee.

Cytoplasmic and nuclear fractionation. S2 cells were washed twice in ice cold PBS, resuspended in solution I (10 mM HEPES, pH 7.9, 10 mM KCl, 0.1 mM MgCl₂, 0.1 mM EDTA, 0.1 mM dithiothreitol (DTT), 0.5 mM phenylmethylsulphonyl fluoride (PMSF) and Roche protease inhibitor cocktail) and passed seven times through a 25G syringe. After centrifugation (2,000 r.p.m. for 10 min at 4 °C), the supernatant was collected as the cytoplasmic fraction. The pellet was washed in solution I four times, resuspended in solution II (10 mM HEPES, pH 7.9, 400 mM NaCl, 1.5 mM MgCl₂, 0.1 mM EDTA, 0.1 mM DTT, 0.5 mM PMSF, 5% glycerol and Roche protease inhibitor cocktail) and incubated on ice for 30 min with occasional flicking. After centrifugation (12,000 r.p.m. for 20 min at 4 °C), the supernatant was collected as the nuclear fraction; 20 μg each sample was analysed by western blotting.

Preparation of the nuclear extract and immunoprecipitation. The nuclear extracts were obtained from S2 cells, and the protein complexes were immunoprecipitated from the extracts, according to ref. 30 with minor modifications. Briefly, for each immunoprecipitation, 300 μl nuclear extract (600–800 μg) was mixed with 300 μl TEA₁₅₀ buffer (10 mM Tris-HCl, pH 8, 150 mM NaCl, 1 mM EDTA, 1 mM DTT, 1 mM PMSF, 0.1% NP40, 2 μg ml⁻¹ leupeptin, 2 μg ml⁻¹ aprotinin, 2 μg ml⁻¹ pepstatin) and 30 μl Protein A/G PLUS-agarose beads (Santa Cruz Biotechnology), and then incubated for 1 h at 4 °C for pre-clearing. The supernatant was transferred to a new tube, and the appropriate amount of one of the following antibodies was added to the supernatant: 5 μg anti-DCR2 (Abcam) and/or 2 μg mouse anti-DCR2 antibody; 2 μg anti-Pol-II antibody (4H8); 10 μl anti-NELF-E antibody; 1–2 μl anti-TBP antibody; or 2 μg rabbit IgG. The samples were incubated for 3 h on a wheel at 4 °C. Then, 40 μl of Protein A/G PLUS-agarose beads was added. After incubation for 2 h, the beads were washed five times with 500 μl of TEA₁₅₀ buffer then resuspended in SDS-PAGE loading buffer and analysed by western blotting. Proteins were detected with the SuperSignal West Dura substrate (Pierce). For single-strand RNase treatment, 2 μl RNase cocktail (RNase A+T1, Ambion) was added during one of the washing steps, and the samples were incubated for 20 min at 30 °C.

RNAi in S2 cells. S2 cells were grown in serum-free insect culture medium (HyQ SFX, HyClone). The production of dsRNAs (400–500 bp) of *EGFP*, *Dcr2* and *Ago2* was performed *in vitro* by T7 transcription. Sense and antisense RNAs were denatured by heating and were re-annealed in water to become dsRNAs. RNAi was performed as described previously³¹ and lasted 8–10 days. The primers for the production of T7 templates were as follows: *EGFP*-F, 5'-ACGTAAACGGCCACAAGTTC-3'; *EGFP*-R, 5'-TGCTCAGGTAGTGGTTCG3'; *DCR2*-F, 5'-GTTCGCTTTGGTCAACAAT-3'; *DCR2*-R, 5'-TGATCGTCTTTCCATGCAG-3'; *DCR2*UTR-F, 5'-ATGATGATCCAGCCAGTC-3'; *DCR2*UTR-R, 5'-TTATTTCGACCAAGGTAAC-3'; *AGO2*-F, 5'-GCTGCAATACTCCAGCACA-3'; and *AGO2*-R, 5'-CTCGGCCTTCTGCTTAATTG-3'.

Antibodies. The mouse anti-RNA Pol II antibody (4H8, Abcam ab5408) recognizes the Ser-5-phosphorylated C-terminal domain³². The mouse anti-RNA Pol II antibody (H5, Covance) recognizes the elongating RNA Pol II, which is phosphorylated at Ser 2 in the C-terminal domain¹⁸. The rabbit anti-DCR1 (ab4735), anti-DCR2 (ab4732), anti-histone H3 (ab1791) and mouse anti-actin (ab8224) antibodies were from Abcam. The mouse anti-β-tubulin antibody (E7) was from the Hybridoma Bank at the University of Iowa. The mouse anti-Flag (M2) antibody was purchased from Sigma. The mouse anti-AGO1, anti-AGO2 and anti-DCR2 antibodies have been described previously^{3,12,13}. The rabbit anti-Pc antibody³³ was provided by R. Paro. The rabbit anti-TBP antibody³⁴ was a gift from J. T. Kadonaga. The anti-NELF-E antibody was described previously¹⁶. In western blotting experiments, a non-commercial anti-DCR2 antibody, kindly provided by Q. Liu³⁵, was also used.

ChIP. Chromatin was prepared as described previously³⁶ from non-treated S2 cells and heat-shocked S2 cells (as described below) with a fixation step of 15–25 min at room temperature. The following antibodies were used for immunoprecipitation (approximately 8 × 10⁶ cells per immunoprecipitation): anti-RNA Pol II (4H8, 2 μl), anti-NELF-E (5 μl), anti-AGO2 (9D6, 3 μl), mouse anti-DCR2 (4 μl) and anti-Flag M2 (as a negative control, 4 μl) antibodies. The specificity of the ChIP-grade anti-AGO2 (9D6) antibody is shown in Supplementary Fig. 6. The anti-DCR2 antibody used for the ChIP experiment is the same one used for the immunofluorescence experiments shown in Supplementary Fig. 1i. Quantitative PCR was performed in a DNA Engine Opticon 2 (MJ Research, Bio-Rad) instrument using the QuantiTect SYBR Green PCR Kit (QIAGEN) or in a LightCycler 480 (Roche) using the Absolute QPCR SYBR Green Mix (Thermo Scientific)

according to manufacturer's instructions. Relative enrichments were calculated as a percentage of the input. The *Hsp70* primer sequences were as follows: the -154 and +58 primers were described previously¹⁸; +471forward, 5'-GATCTGGCACCACCTACTC-3'; +471reverse, 5'-TGGGAGTCGTTGAAGTAGGC-3'; +2171forward, 5'-CACGATCAAGAACGACAAGG-3'; and +2171reverse, 5'-CTTTGGCCTTAGTCGACCTC-3'. The names of the primer pairs indicate the distance of the middle of each amplicon from the *Hsp70* transcription start site.

Heat-shock induction. Third-instar larvae were transferred to preheated 1.5-ml microcentrifuge tubes and submerged in a 37 °C water bath for 40 min. S2 cells were transferred to pre-heated medium and submerged in a 37 °C water bath for 40 min.

Quantitative RT-PCR analysis. Total RNA from S2 cells or larvae was isolated with TRIzol reagent (Invitrogen). RNA from each sample was subjected to cDNA synthesis using a QuantiTect Reverse Transcription Kit (QIAGEN). All primers were annealed at 60 °C. Quantitative PCR was performed with a DNA Engine Opticon 2. Quantification was normalized to the housekeeping gene *GAPDH1*, and relative expression levels were calculated using the following equation: $A = 2^{[Ct(ref) - Ct(ref - control)] - [Ct(sample) - Ct(sample - control)]}$. The primer sequences were as follows: *GAPDH1*-F, 5'-ATCGTCGAGGGTCTGATGAC-3'; *GAPDH1*-R, 5'-ACCGAAGCTGTTGTCGTACC-3'; *HSP70*, see +471 primers in the ChIP section; *HSP70A*-F, 5'-GTGTCTACCAACATGGCAAG-3'; *HSP70A*-R, 5'-CTGTGTTCTGGGGTTCATG-3'; *HSP70B*-F, 5'-GGTTGAGATTATCGCCAATGAC-3'; *HSP70B*-R, 5'-GTCGTATTTTCGGCCGATGAG-3'; *HSP68*-F, 5'-GAAGGCACTCAAGGACGC-3'; *HSP68*-R, 5'-GAAGGTCTTGGACTGCTTGC-3'; *MFAS*-F, 5'-AGAAACCGTGGACACCTTTG-3'; *MFAS*-R, 5'-TGTGAGTCAAGCGTTTCTGG-3'; *CG9008*-F, 5'-GTTGGCAGAACATCGAAGG-3'; *CG9008*-R, 5'-AGCGCAGCTTGAGTTTTTGT-3'; *RHO*-F, 5'-CGCGAGATCA TCAAACCTGAG-3'; *RHO*-R, 5'-CTCGTAAATCCAGGAGCTG-3'; *FZ*-F, 5'-GTCAGCGTATGCCCTACCAT-3'; *FZ*-R, 5'-ACTTTTTCGCACGGGACTTA-3'; *AGO2*-F, 5'-CTGGATGATGGATACGAGGC-3'; *AGO2*-R, 5'-GCGACTGTGGAAGTAGGACG-3'; *DCR2*-F, 5'-GCAATAGCGATGCAATGAG-3'; *DCR2*-R, 5'-CGTCTAGAGAAGGCATCG-3'; *AUB*-F, 5'-AAACCAACTGGCTGATGTC-3'; and *AUB*-R, 5'-GCTCTGCAAGGTAATAACG-3'.

FISH analysis. Cytological preparations and FISH were carried out as described previously³⁷. FISH signals were quantified by densitometric analysis using QFluoro software (Leica). Any deviation of 33% or greater from the normal average relative puffing ratio of the 87C locus to the 87A locus in wild-type flies was considered an increase in puffing at the 87C locus relative to the 87A locus in the *Ago2* and *Dcr2* mutants analysed.

Immunostaining of salivary gland polytene chromosomes. Polytene chromosomes were prepared from third-instar larvae grown at 18 °C. Single and double immunostaining was carried out as described previously³⁸. The Fab-fragment blocking method was used to stain the chromosomes with anti-AGO2 and anti-RNA Pol II antibodies, both raised in mice. Antibodies were used at the following dilutions: anti-RNA Pol II antibody (H5), 1:200; anti-AGO2 antibody, 1:50; anti-AGO2 antibody (9D6), 1:50; mouse anti-DCR2 antibody, 1:100; and Fab fragment (anti-mouse), 1:100. Given the specificity of the anti-AGO2 and anti-DCR2 antibodies in polytene staining, the cytoplasmic and nucleoplasmic background signals were removed (using the Lasso tool in Photoshop; Adobe), to highlight AGO2 and DCR2 chromatin binding.

Permanganate footprinting. S2 cells (2 ml, approximately 4 × 10⁶ cells ml⁻¹) were treated with permanganate, essentially as described previously¹⁹. The permanganate cleavage pattern was analysed as described previously³⁹. The primer sequences were as follows: *CG9008*+237R_LM1, 5'-CGCATTTACATAATGTTTGC-3'; *CG9008*+226R_LM2, 5'-AATGTTTGCAAAAATTATTCTGC-3'; *CG9008*+220R_LM3, 5'-TGCAAAAATTATTCTGCACACAAG-3'; *FZ*+212R_LM1, 5'-AAGTACCGTTAGCTGTATATCAT-3'; *FZ*+213R_LM2, 5'-TTAGCTGTATATCATTTATGCCTCC-3'; *FZ*+197R_LM3, 5'-TATGCCTCCCGCTT-3'; *MFAS*+178_LM1, 5'-TTATTGTCAATTGTCTTGTTTTTTAC-3'; *MFAS*+159_LM2, 5'-TTTTACAAAAATTGGCACACACT-3'; *MFAS*+155_LM3, 5'-ACAAA AATTGGCACACACTCAATTA-3'; *RHO*+210R_LM1, 5'-CTTAGTTTTGCTGCTCGTAA-3'; *RHO*+204R_LM2, 5'-TTTGCTGCTGTAATCCA-3'; *RHO*+198R_LM3, 5'-GCTCGTAAATCCAGGAGCTGT-3'; for *HSP70* 87A, 87C/A250_LM1, 5'-GCAGGCATTGTGTGTGAGT-3'; 87C250_LM2, 5'-GGCATTGTGTGTGAGTTCTTCTTT-3'; 87C250_LM3, 5'-TGTGTGAGTTCTTCTTCTCGTAACTTG-3'; linker A', 5'-GCGGTGATTTAAAAGATCTGAA TTC-3'; and linker B, 5'-GAATTCAGATC-3'. LM1 was the first primer used in each set. LM2 was used for amplification. LM3 was used for labelling. Linker A' and linker B are the two primers that are annealed and ligated to the blunt ends generated by primer extension with LM1. Quantification of the autoradiographs was carried out using ImageQuant software (Bio-Rad).

DCR2-Flag rescue assay. To selectively inhibit the endogenous *Dcr2* gene, a specific dsRNA targeting the 3'-untranslated region sequence missing in the

Dcr2-Flag transgene was used. After 8 days of dsRNA treatment, the expression of the fusion protein was induced by adding 1 mM CuSO₄.

Chromatin-binding assay. The chromatin-binding assay protocol was essentially as described previously¹¹. S2 cells (60 ml, approximately 3–6 × 10⁶ ml⁻¹) were washed with cold PBS. One-tenth of the cell suspension (control fraction, C) was resuspended in RIPA buffer (150 mM Tris-HCl, pH 8.0, 150 mM NaCl, 0.5% DOC, 0.1% (w/v) SDS, 1% (v/v) NP-40, 2 μg ml⁻¹ leupeptin, 2 μg ml⁻¹ aprotinin, 2 μg ml⁻¹ pepstatin, 1 mM PMSF, 1 mM NaF and 1 mM sodium orthovanadate) and left for 30 min on ice. The remaining fraction was lysed for 15 min on ice in cold CSKI buffer (10 mM PIPES, pH 6.8, 100 mM NaCl, 1 mM EDTA, 300 mM sucrose, 1 mM MgCl₂, 1 mM DTT, 0.5% (v/v) Triton X-100, 2 μg ml⁻¹ leupeptin, 2 μg ml⁻¹ aprotinin, 2 μg ml⁻¹ pepstatin, 1 mM PMSF, 1 mM NaF and 1 mM sodium orthovanadate). The cell lysate was divided into two portions, which were centrifuged at 500g at 4 °C for 3 min. The supernatants (S1 fraction), which contain Triton-soluble proteins, were further analysed. One of the pellets was washed twice in CSKI buffer and then resuspended in RIPA buffer (the P1 fraction). The second pellet, after washing in CSKI buffer, was resuspended in CSKII buffer (10 mM PIPES, pH 6.8, 50 mM NaCl, 300 mM sucrose, 6 mM MgCl₂, 1 mM DTT, 2 μg ml⁻¹ leupeptin, 2 μg ml⁻¹ aprotinin, 2 μg ml⁻¹ pepstatin, 1 mM NaF and 1 mM sodium orthovanadate), then treated with DNase (Promega) for 30 min and extracted with 250 mM NH₄SO₄ for 10 min at 25 °C. The sample treated with DNase and salt was then centrifuged at 1,200g for 6 min at 4 °C, and the supernatant (S2 fraction) and pellet (P2 fraction) were collected. The P2 fraction was also resuspended in RIPA buffer. All fractions (20 μg) were analysed by western blotting.

Purification of AGO2-associated RNAs. For heat shock, S2 cells were transferred to pre-heated medium at 37 °C and submerged in a 37 °C water bath for 40 min. Immunoprecipitation was performed as described previously³. Briefly, S2 cells were washed twice in ice cold PBS, resuspended in an EMPIGEN-containing PBS buffer (1% EMPIGEN, 1 mM EDTA, 100 mM DTT, 2 μg ml⁻¹ pepstatin, 2 μg ml⁻¹ leupeptin and 0.5% aprotinin) and incubated on ice for 10 min to lyse cells. After centrifugation (15,000 r.p.m. for 20 min at 4 °C), the supernatant was collected. Immunoprecipitation was performed using an anti-AGO2 antibody (9D6) or mouse non-immune IgG (negative control) immobilized on GammaBind beads (GE Healthcare). The reaction mixture was rocked at 4 °C for 2 h and washed five times with EMPIGEN-containing PBS buffer.

For silver staining, the washed beads were incubated with 2× sample buffer (20% glycerol, 100 mM Tris-HCl, pH 6.8, 4% SDS and 0.02% bromophenol blue) for 10 min at room temperature, and DTT (200 mM final concentration) was added to the mixture. The sample was then incubated at 95 °C for 5 min and resolved by SDS-PAGE. After electrophoresis, the protein bands were visualized by SilverQuest (Invitrogen).

The small RNAs associated with AGO2 were treated with phenol:chloroform and precipitated with isopropyl alcohol. The RNAs were then dephosphorylated with calf intestinal alkaline phosphatase (New England BioLabs), labelled with [³²P]ATP with T4 polynucleotide kinase (New England BioLabs) and resolved on a 12% polyacrylamide denaturing gel.

Small RNA library sequencing and computational analysis. Small RNA libraries were prepared as described previously⁴⁰ with one of two barcodes attached to the libraries generated from the immunoprecipitation experiments, regardless of the presence or absence of heat shock. The libraries were sequenced using a Genome Analyzer IIx (Illumina) in two lanes. Linkers and barcode sequences were extracted from the raw tags; the tags were mapped to the *Drosophila* dm3 genome assembly using the program Nexalign⁴¹. The genome classification of individual tags was determined by overlap with existing definitions culled from publicly available genome tracks in FlyBase and functional RNA databases^{42,43}. Tags that mapped

to more than ten locations in the genome were removed from subsequent analyses; tag counts for the remaining tags were distributed evenly across the total number of mapping sites. Tags were normalized to tags per million before comparisons across libraries. A summary of the basic statistical parameters for the four libraries is provided in Supplementary Table 3. The extraction rates were between 70% and 75% per library (data not shown); mapping rates were above 90% (Supplementary Table 3).

As an additional normalization strategy, the tags per million microRNA count was also tabulated for each library (Supplementary Table 5) because microRNA percentages were largely unaffected by heat-shock treatment (Supplementary Fig. 12); fold enrichments calculated across conditions with these values were consistent with tags per million normalization (data not shown). Sense-antisense distinctions were decided according to FlyBase gene definitions; overlapping gene definitions on the same strand were merged, and the tags mapping to overlapping sense-antisense transcripts were included in both sense and antisense totals. Clusters of CAGE tags, which are representative of transcription start site activity, were linked to heat-shock loci using 5' and 3' FlyBase gene definitions; each locus was visually inspected in a genome browser, and the gene definitions were adjusted to account for differences in transcription start sites between embryonic tissue and FlyBase gene definitions. Large-scale genome comparisons were carried out using the BEDTools utilities suite⁴⁴.

30. Lupo, R., Breiling, A., Bianchi, M. E. & Orlando, V. *Drosophila* chromosome condensation proteins Topoisomerase II and Barren colocalise with Polycomb and maintain Fab-7 PRE silencing. *Mol. Cell* **7**, 127–136 (2001).
31. Breiling, A., Turner, B. M., Bianchi, M. E. & Orlando, V. General transcription factors bind promoters repressed by Polycomb group proteins. *Nature* **412**, 651–655 (2001).
32. Stock, J. K. *et al.* Ring1-mediated ubiquitination of H2A restrains poised RNA polymerase II at bivalent genes in mouse ES cells. *Nature Cell Biol.* **9**, 1428–1435 (2007).
33. Messmer, S., Franke, A. & Paro, R. Analysis of the functional role of the Polycomb chromo domain in *Drosophila melanogaster*. *Genes Dev.* **6**, 1241–1254 (1992).
34. Hsu, J. Y. *et al.* TBP, Mot1, and NC2 establish a regulatory circuit that controls DPE-dependent versus TATA-dependent transcription. *Genes Dev.* **22**, 2353–2358 (2008).
35. Liu, Q. *et al.* R2D2, a bridge between the initiation and effector steps of the *Drosophila* RNAi pathway. *Science* **301**, 1921–1925 (2003).
36. Breiling, A., O'Neill, L. P., D'Eliseo, D., Turner, B. M. & Orlando, V. Epigenome changes in active and inactive Polycomb-group-controlled regions. *EMBO Rep.* **5**, 976–982 (2004).
37. Pimpinelli, S., Bonaccorsi, S., Fanti, L. & Gatti, M. in *Drosophila: A Laboratory Manual* (eds Sullivan, W., Ashburner, M. & Hawley, S.) 1–24 (Cold Spring Harbor Laboratory Press, 2000).
38. Corona, D. F., Armstrong, J. A. & Tamkun, J. W. Genetic and cytological analysis of *Drosophila* chromatin-remodeling factors. *Methods Enzymol.* **377**, 70–85 (2004).
39. Cartwright, I. L. *et al.* Analysis of *Drosophila* chromatin structure *in vivo*. *Methods Enzymol.* **304**, 462–496 (1999).
40. Kawano, M. *et al.* Reduction of non-insert sequence reads by dimer eliminator LNA oligonucleotide for small RNA deep sequencing. *Biotechniques* **49**, 751–755 (2010).
41. de Hoon, M. J. *et al.* Cross-mapping and the identification of editing sites in mature microRNAs in high-throughput sequencing libraries. *Genome Res.* **20**, 257–264 (2010).
42. Tweedie, S. *et al.* FlyBase: enhancing *Drosophila* Gene Ontology annotations. *Nucleic Acids Res.* **37**, D555–D559 (2009).
43. Mituyama, T. Y. K. *et al.* The Functional RNA Database 3.0: databases to support mining and annotation of functional RNAs. *Nucleic Acids Res.* **37**, D89–D92 (2009).
44. Quinlan, A. R. & Hall, I. M. BEDTools: a flexible suite of utilities for comparing genomic features. *Bioinformatics* **26**, 841–842 (2010).